INFLUENCE OF INHIBITOR BINDING ON THE INTERNAL MOTIONS OF LYSOZYME

ALBERT J. CROSS AND GRAHAM R. FLEMING
Department of Chemistry and the James Franck Institute, University of Chicago, 5735 S. Ellis Avenue, Chicago, Illinois 60637

ABSTRACT Time-resolved laser-induced fluorescence depolarization measurements of internal motions in lysozyme are presented. The fluorescent dye eosin binds in a one-to-one complex with the enzyme, and is used both to measure the overall tumbling time constants and to probe the motions of residues in the region of binding. The precision and accuracy of the present method for determining the overall tumbling time constants compare favorably with those from other methods used in the literature. The extent of the internal motions, as described by a model independent order parameter, S^2, is temperature dependent, and changes when the inhibitor *N,N',N''*-triacetylchitotriose, $(GlcNAc)_3$, is bound to the active site of the enzyme. The observed temperature dependence and changes in S^2 upon binding of $(GlcNAc)_3$ are interpreted in terms of a nonharmonic model of the effective potential that is consistent with the picture of concerted motions in the protein. The values of the parameters of the potential that reproduce the data with and without the bound inhibitor imply that $(GlcNAc)_3$ binding causes an increase in the rigidity of the protein, which agree qualitatively with other results on the lysozyme-$(GlcNAc)_3$ system.

INTRODUCTION

Motions of residues in the interior regions of proteins have been suggested as an important kind of dynamics that may play an essential role in biological activity (1–9). One would like to obtain a detailed description of the motions of individual residues, and learn the contribution of these motions to protein function. Molecular dynamics calculations can provide in principle these details, but only within the limitations of the assumption of particular intermolecular potentials, small system sizes (often neglecting the effect of hydration of the protein) and finite trajectory times which may not sample sufficiently over all accessible regions of phase space. Information provided by experiments generally is in the form of moments of distribution functions, and thus necessarily represents averages over some features of interest. Although some details are averaged out, experimental results can provide data by which various simple models of the motions are judged, particularly when such models predict experimental observations that can be confirmed or denied.

Time-resolved fluorescence anisotropy is one of several methods that have been applied to the study of internal and overall tumbling motions in proteins (10, 11). In this work, we apply the technique to measure internal motions in the hydrophobic box region (12, 13) of lysozyme (14) using an extrinsic probe, the dye eosin, which binds to this region of the enzyme (15, 16). The hydrophobic box region is adjacent to, but distinct from, the active site of the protein. These measurements provide evidence that the hydrophobic box residues undergo significant motions on the timescale of 100 ps or less. This is in accord with x-ray crystallography measurements of atomic mean square displacements that show larger than average mobilities for the atoms in this region of lysozyme (7).

We find that the extent of the motions varies significantly over the temperature range of 5° to 65°C, and that the observed temperature dependence is altered when the inhibitor *N,N',N''*-Triacetylchitotriose (17), $(GlcNAc)_3$, is bound simultaneously to the active site.

These motions are interpreted in terms of the model-independent order parameter (18), S^2, which is a measure of the extent of restriction of the motions of the probe molecule. Values of S^2 can be computed from models for the restricted motions that give the probability distribution function for orientation of the measurement vector associated with the probe molecule with respect to a coordinate system fixed to the body of the protein. In the case of fluorescence, this vector is the transition dipole. Unfortunately, a single value of S^2 does not uniquely determine a probability distribution, so one must rely on additional information to judge which models for the restricted motion are appropriate.

One model of restricted motions that has been used in interpreting S^2 data is the free motion within a cone (10, 18–20). In this model, one has the simplest probability distribution: a constant for θ (the angle that the vector

Dr. Fleming is an Alfred P. Sloan Foundation Fellow and Camille and Henry Dreyfus Teacher Scholar. Dr. Cross' current address is Department of Chemistry, B-014, University of California at San Diego, La Jolla, CA 92093.

makes with an assumed symmetry axis fixed to the protein) less than a fixed θ_0 (the cone semiangle), and zero otherwise. There is a one-to-one mapping of θ_0 (from 0–90°) to S^2 values, which is given by a simple relation. Thus, interpretation in terms of the cone model transfers data from the domain of S^2 to that of θ_0. While this can make it easier to visualize the extent of the restricted motion, strict confinement within a cone may not be the underlying probability distribution, in which case the cone model for the potential is not really appropriate.

In the absence of additional information, the cone model is as good as any for use in interpreting a particular S^2 value, but in this work since we have S^2 values measured over a temperature range, and under two conditions (with and without the bound inhibitor), we explore the possibility of a potential model that is consistent with the observed data, and from which the observed trends with temperature and changes upon inhibitor binding naturally arise. While for the cone model, a temperature dependence in S^2 is simply interpreted as a change in the cone semiangle (and thus the potential) with temperature, we suggest here that a potential model, which is temperature independent but gives rise to a temperature dependence in S^2 due to Boltzmann activation, may be more appropriate for the case of lysozyme. Our model of the effective potential is consistent with the picture of concerted motions in the protein. The values of the parameters of the potential that reproduce the data with and without the bound inhibitor imply that $(GlcNAc)_3$ binding causes an increase in the rigidity of the protein, which agrees qualitatively with other results on the lysozyme $(GlcNAc)_3$ system (21, 22).

EXPERIMENTAL

Materials

$(GlcNAc)_3$ and lysozyme were obtained from Sigma Chemical Co. (St Louis, MO) and used without further purification. Eosin was purified by thin layer chromatography (TLC) as described previously (14).

Concentrations of the three compounds had to be chosen carefully to insure that most of the eosin was bound to lysozyme, most of the lysozyme had $(GlcNAc)_3$ bound to it, and that little of the lysozyme formed dimers. The concentrations used were: lysozyme, $1.2 \cdot 10^{-4}$ M; eosin, $3.8 \cdot 10^{-6}$ M; $(GlcNAc)_3$, $6.4 \cdot 10^{-4}$ M. Concentrations of lysozyme and eosin were determined spectroscopically as before (14); $(GlcNAc)_3$ concentration was determined by dissolving a known weight into known volume. We have shown previously that with the concentrations of eosin and lysozyme used, essentially all of the eosin is bound to the lysozyme over the experimental temperature range (14). It is essential that all eosin present be bound to the enzyme, as unbound eosin reorients very rapidly, and emission from it could be misinterpred as motion with respect to the protein. As in the previous study, the pH of the solutions was 5.3.

Methods

Polarized fluorescence emission curves were obtained by time-correlated, single-photon counting (23, 24), using the experimental arrangement described previously (14, 25). The excitation source consisted of an actively mode-locked Ar^+ ion laser (Coherent CR-6) operating at a wavelength of 514.5 nm. Emission from the samples were passed through glass cutoff filters (≥580 nm) to remove scattered excitation light.

Polarized emission data was analyzed by simultaneous fitting of parallel and perpendicular polarized decay curves using the method previously described (25). The time range of fitting used was ~8 ns, and started ~2 ns after the excitation pulse. For a set of four fluorescence emission curves, two each of parallel and perpendicular emission, fitted values of $r(0^+)$, the extrapolated value of $r(t)$ at zero time from a fit to the latter part of the decays, and τ_r, the overall reorientation time constant, were obtained. The fitted $r(0^+)$ values were divided by $r(0)$ to calculate S^2 (see Theory section). We have previously shown that within our experimental error $r(0) = 0.40$ for eosin (25).

THEORY

The time-resolved emission anisotropy, $r(t)$, is related to a correlation function of the transition dipole moment in the laboratory frame. For a spherical body that undergoes isotropic rotational diffusion, $r(t)$ decays as a single exponential. For an asymmetric ellipsoid of revolution, $r(t)$ can decay with as many as five exponential terms (26–29), while for a symmetric ellipsoid, there are in general three exponential terms in $r(t)$. We have previously calculated the decay constants that would be obtained for a symmetric ellipsoid that approximates the shape of lysozyme (14), and in view of these calculations, it is unlikely that the anisotropic components in the overall tumbling of the protein would be resolved by the measurements presented here.

If there is a rapid restricted motion of the chromophore in addition to the overall rotation of the macromolecule to which it is attached, $r(t)$ in general decays nonexponentially, and can be approximated as a sum of two exponential decays. In this case, the extrapolation of $r(t)$ back to zero time gives a value $r(0^+)$, which is less than the true initial value, $r(0)$. The extent of the restricted motion can be described by the order parameter (14, 18), S^2, which is given by

$$S^2 = \frac{r(t)}{r(0)} e^{+t/\tau_r} = \frac{r(0^+)}{r(0)}. \quad (1)$$

If S^2 is unity,the chromophore is fixed with respect to the body of the protein; values less than one indicate that some restricted motion is occurring. The constant associated with the decay of $r(0)$ to $r(0^+)$ is related to the correlation time for various orientations that the dye can have within the hydrophobic box region.

Models for the restricted motion can be used to predict S^2 values that are then compared with experiment. The general approach is as follows. A potential of mean force, $V(\theta)$, is assumed to give the energy as a function of the angle that the chromophore makes with respect to a symmetry axis, fixed with respect to the body of the protein. This potential represents the energy of the system with the probe vector at a particular θ averaged over an ensemble of relaxed configurations of the rest of the protein.

While the motion of eosin is probably not precisely axially symmetric, the experimental data available do not justify a more complex model of the motion. If the

structure of the complex were known, for example from crystallographic measurements, then it would be of interest to explore models that had anisotropic motion about an axis.

If one assumes that the shape of the potential is temperature independent, the probability of finding the probe at θ is determined by a Boltzmann factor. Following Lipari and Szabo, the expression for $S(T)$ is then

$$S = \langle P_2(\cos\theta)\rangle, \tag{2}$$

or

$$S(T) = \frac{\int_0^\pi P_2(\cos\theta)\exp\left(\frac{-V(\theta)}{k_bT}\right)\sin\theta\,d\theta}{\int_0^\pi \exp\left(\frac{-V(\theta)}{k_bT}\right)\sin\theta\,d\theta}. \tag{3}$$

The temperature dependence of $S(T)$ arises solely from Boltzmann activation in the temperature-independent potential $V(\theta)$.

Setting aside the cone model, which has no intrinsic temperature dependence, perhaps the simplest model is motion of the eosin in a harmonic potential. Previously we have given the analytical solution to this problem and demonstrated that the temperature dependence of this model is much too weak to fit the lysozyme-eosin (LE) data (14). Motivated, in part, by the interesting discussion of Gavish (30) on modeling the unusual temperature dependence of mean square displacements of atoms in proteins by nonharmonic potentials, we studied the temperature dependence of the order parameters generated from the following nonharmonic potential

$$V(\theta) = \begin{cases} 0 & \text{if } 0 \le \theta < \theta_0 \\ V_0 + V_1\dfrac{(\theta-\theta_0)^2}{(\pi-\theta_0)^2} & \text{if } \theta_0 \le \theta \le \pi \end{cases}. \tag{4}$$

The harmonic dependence after θ_0 was included to prevent the vector from making nonphysical excursions far beyond θ_0. The order parameter cannot be evaluated in closed form, but can be related to finite integrals of Gaussian damped sines and cosines, which are in turn related to the error function of a complex argument

$$\begin{aligned} S(T) = {} & \frac{(1-\cos^3\theta_0)}{2\Gamma} + \frac{e^{-V_0/k_bT}}{8\Gamma} \\ & \cdot\left[\cos 3\theta_0\, G^s\left(3\pi - 3\theta_0, \frac{\lambda}{9k_bT}\right)\right. \\ & + \sin 3\theta_0\, G_C\left(3\pi - 3\theta_0, \frac{\lambda}{9k_bT}\right) \\ & + 3\cos\theta_0\, G^s\left(\pi-\theta_0, \frac{\lambda}{k_bT}\right) \\ & \left. + 3\sin\theta_0\, G_C\left(\pi-\theta_0, \frac{\lambda}{k_bT}\right)\right] - \frac{1}{2}, \end{aligned} \tag{5}$$

where

$$\Gamma = (1-\cos\theta_0) + e^{-V_0/k_bT} \cdot\left[\cos\theta_0\, G^s\left(\pi-\theta_0, \frac{\lambda}{k_bT}\right) + \sin\theta_0\, G_C\left(\pi-\theta_0, \frac{\lambda}{k_bT}\right)\right] \tag{6}$$

$$\lambda = \frac{V_1 - V_0}{(\pi-\theta_0)^2} \tag{7}$$

$$G^s(\theta,\alpha) = \int_0^\theta \theta^{-\alpha x^2}\sin x\,dx = \exp\left[-\frac{1}{4\alpha}\right]\cdot\frac{1}{2}\cdot\sqrt{\frac{\pi}{\alpha}} \cdot \text{im}\left\{erf\left(\sqrt{\alpha\theta} - \frac{i}{2\sqrt{\alpha}}\right) + erf\left(\frac{+i}{2\sqrt{\alpha}}\right)\right\} \tag{8}$$

$$G_C(\theta,\alpha) = \int_0^\theta e^{-\alpha x^2}\cos x\,dx = \exp\left[-\frac{1}{4\alpha}\right]\cdot\frac{1}{2}\cdot\sqrt{\frac{\pi}{\alpha}}\cdot Re\left\{erf\left(\sqrt{\alpha\theta} - \frac{i}{2\sqrt{\alpha}}\right)\right\}. \tag{9}$$

It can be shown that this expression for $S(T)$ reduces to the correct limits for a harmonic potential, i.e., when we take $\theta_0 \to 0$, we obtain a previously given expression (14). In the previous work, the limits of integration were extended from π to ∞ to simplify the calculation.) Also, the cone model expression is obtained in the limit $V_1 \to \infty$. Numerical calculations of S(T) for given values of the three parameters were made by using a series expansion and asymptotic formula for $erf(Z)$.[31]

RESULTS

Overall Tumbling of the Complex

Time-resolved fluorescence depolarization provides a direct measurement of the orientational relaxation of large molecules, and is a particularly convenient method provided that the fluorescing probe has a lifetime within an order of magnitude of τ_r. Fig. 1 gives τ_r as a function of

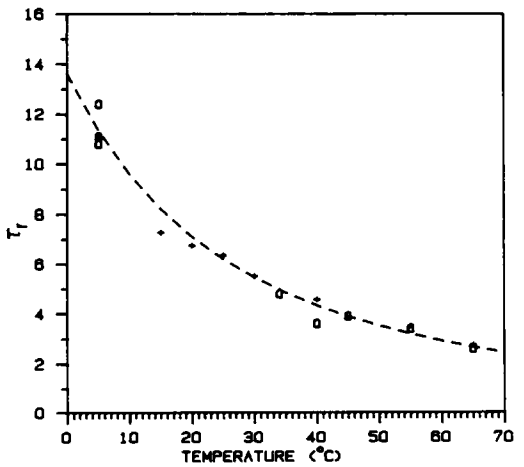

FIGURE 1 Overall rotational motion from asymptotic fits to eosin-lysozyme (O) and eosin-lysozyme-$(GlcNAc)_3$ (+) data. The dashed line assumes $\tau_r \propto \eta/T$, with proportionality constant determined by the average value of τ_r at 5°C (see text).

temperature for both the eosin-lysozyme (LE) and eosin-lysozyme-$(GlcNAc)_3$ (LEN_3) data. We found that the binding of $(GlcNAc)_3$ to lysozyme does not substantially alter the overall tumbling motion. The similarity of LE and LEN_3 data in Fig. 1 also implies that binding of $(GlcNAc)_3$ does not displace the eosin from the enzyme.

The dashed curve in Fig. 1 was obtained by assuming Stokes-Einstein behavior for the τ_r values, i.e., assuming that they scale as η/T, using the following procedure. The values of τ_r at 5°C for both LE and LEN_3 data were averaged to obtain 11.35 ns. This τ_r was used with the Einstein law (26) to calculate the effective volume of a sphere that would give rise to that rotation time. The volume so calculated was 29,000 Å^3, which is close to the volume of an ellipsoid that approximates the shape of lysozyme (7) (with semiaxes 15 × 15 × 22.5 Å), 21,200 Å^3. The curve was generated assuming that this calculated effective volume remains constant over the experimental temperature range, and agrees well with the data at higher temperatures. Note that this is not a fit to all of the data in Fig. 1, but represents the extrapolation asuming Stokes-Einstein behavior from the average value at 5°C. The excellent fit to Stokes-Einstein behavior implies that there is no gross structural change occurring with increasing temperature, which is consistent with other observations (32).

Our values for the rotation time (e.g., 7 ns at 20°C, 0.12 mM) are significantly lower than most NMR determinations that use higher concentrations of the enzyme. In particular, Schramm and Oldfield (33) give values of 20 ns (13 mM, 40°C) and 30 ns (13 mM, 22°C). Wilbur and co-workers (34) report two values measured at different magnetic field strengths, both being higher than our result: 19 ns (14.6 mM, 43°C, 14.2 kG) and 8 ns (14.6 mM, 43°C, 63.4 kG). However, as we noted in our previous study (14), our results are in reasonable agreement with NMR measurements of Dill and Allerhand (35): 7.5 ns (7 mM, 20°C) and 3.8 ns (7 mM, 60°C). Wooten and Cohen (36) made nmr measurements of the rotation time of lysozyme with and without $(GlcNAc)_3$ bound. For lysozyme at 25°C they obtained 22.6 ns (pH 4.2, 11 mM), 27.1 ns (pH 7.2, 11 mM), 13.3 ns (pH 4.3, 7 mM), and 21.3 ns (pH 7.3, 7 mM). They attributed the trends in these values to dimerization at higher concentrations and pH values. When $(GlcNAc)_3$ was bound, they obtained (again at 25°C) 5.7 ns (pH 4.2, 7 mM) and 7.5 ns (pH 7.5, 7 mM). They interpreted this as showing that addition of the inhibitor caused disaggregation of the lysozyme. Again, in light of this it seems unlikely that there is significant dimerization of the enzyme in the concentrations used in this work.

We believe that the differences between our measurements and those using NMR is due in large part to dimerization and alteration of the solvent viscosity at high enzyme concentrations. Also, extraction of rotation times from NMR experiments requires an assumption about the bond lengths associated with the measured nuclei. In our measurements, provided that one is certain that all of the probe molecules are attached to the enzyme, no assumptions are necessary to obtain rotation times from the polarized emission curves. We view the disparity of times obtained at different magnetic field strengths as indicate of the magnitude of uncertainty in the NMR measurements. In view of these results, further work is needed to clarify the connection between measurements of τ_r obtained by different techniques.

Internal Motions in Lysozyme

The experimental values of S^2 for LE and lysozyme LEN_3 are given in Fig. 2. The order parameters extracted from experiment are model-independent but can be compared with predictions from various models of the motion.

The ability of the potential in Eq. 4 to describe our data was examined by conducting a grid search of the three dimensional parameter space for sets of parameter values that reproduced the end points of the $S^2(T)$ curves. The criterion for fitting was that the calculated values of S^2 at 0° and 70°C were within 0.02 of the S^2 values of the linear least-squares fits to the data. Since there are three parameters it might be expected that many sets would give satisfactory fits. A special case of this potential with V_0 set to zero was tried initially but like the (unshifted) harmonic potential, it produced a much too weak temperature dependence regardless of the value of V_1. In fact, a single cluster of parameters produced a fit for each data set (LE or LEN_3). No other satisfactory fits could be found outside of these two clusters in an extensive search of parameter space. The LE and LEN_3 clusters for the V_0 and θ_0 are shown in Fig. 3. The average values of V_0 are 2.8 ± 0.3 kcal/mol (LE) and 3.6 ± 0.2 kcal/mol (LEN_3, and of θ_0 are 8° ± 3° (LE) and 6° ± 2° (LEN_3).

Although it was possible to fit the data with parameter sets, where $V_0 = V_1$, we eliminated these on the physical

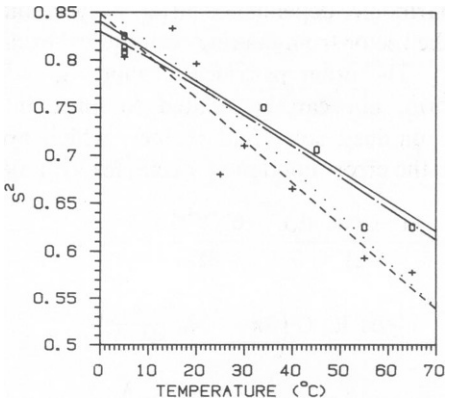

FIGURE 2 S^2 vs. temperature for the lysozyme-eosin (O) and lysozyme-eosin-$(GlcNAc)_3$ (+). Linear least-squares fits to LE (—) and LEN_3 (— —) are shown. Also illustrated are curves generated from representative parameters (see text) for the nonharmonic potential, Eq. 4. For LE (— ·), the curve shown has θ_0 = 8.37°, V_0 = 2.63 kcal/mol, V_1 = 16.11 kcal/mol; for LEN_3 (· · ·), the curve shown as θ_0 = 4.79°, V_0 = 3.61 kcal/mol, and V_1 = 11.58 kcal/mol.

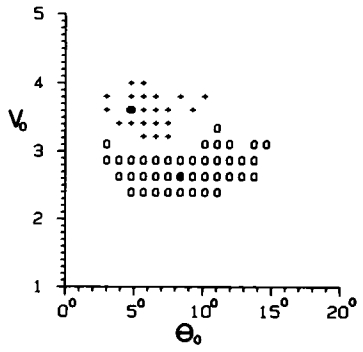

FIGURE 3 Values of V_0 and θ_0 found in the grid search of the parameter space of the nonharmonic potential that fit the LE (O) and LEN_3 (+) data. The criterion for fitting was that the calculated values of S^2 at 0° and 70°C were within 0.02 of the S^2 values of the linear least-squares fits to the data. The values of V_1 (not illustrated) were 18 ± 6 kcal/mol (LE) and 10 ± 3 kcal/mol (LEN_3). The two marked points are those used to generate the representative curves in Fig. 2.

grounds that the probability of finding the vector must fall off at large θ. Values of V_1 in the parameter sets shown in Fig. 3 had a larger variance than those of V_0, since the fits to the data do not determine V_1 very well. Because of this, and since V_1 was primarily introduced to provide a finite force constant for the potential around θ_0, we do not feel it useful to attach quantitative significance to the particular values of V_1.

DISCUSSION

We interpret the potential of Eq. 4 by means of Fig. 4 as follows. The probe molecule can move unhindered over the range 0–θ_0. Further motion requires energy accumulation in collective modes of the protein corresponding to a concerted motion. After accumulation of V_0 in the collective mode(s), the vector can again move in a direction with increasing θ, and its motion becomes relatively unrestricted with an approximately harmonic restoring force. The projection of the multidimensional reaction coordinate onto one dimension, i.e., θ, produces the potential of Eq. 4.

Use of a temperature-independent potential for restricted motions in lysozyme makes sense in light of two observations. First, the gross structure of lysozyme does not change much over the experimental temperature range (32). Our measurements support this as the fit to Stokes-Einstein behavior over the experimental temperature range implies that the effective volume of the molecule is constant. However, application of the cone model would require a variation in θ_0 from 18° to 32° over the temperture range of 0–70°C for the LE data (more for the LEN_3 data), which probably would correspond to a significant structural change. In contrast, our model assumes a constant potential, with increases in temperature causing an increase in the extent of fluctuations around the average structure.

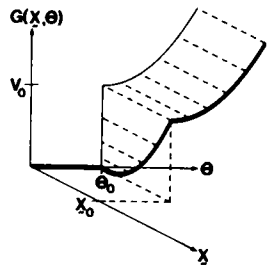

FIGURE 4 Schematic illustration of the interpretation of the nonharmonic potential defined by Eq. 4 in multidimensional coordinate space. The vertical axis gives the free energy, G. The angle of the transition dipole with respect to a protein fixed axis is given by θ. The coordinate x represents additional modes of the protein into that energy must be channeled before movement to angles $>\theta_0$ can occur. The dark line shows a path in the space whose projection on the G, θ plane gives the one-dimensional nonharmonic potential of Eq. 4.

Second, molecular dynamics calculations of an α-helical polypeptide over a range of temperatures showed significant deviation from harmonic behavior (37) implying that nonharmonic potentials may be necessary to describe motions of even the simplest of proteins.

Hydrogen exchange experiments on lysozyme with GlcNAc bound were interpreted in terms of an increase in the activation energy required for dynamic fluctuations of the enzyme and it was concluded that the changes were propagated throughout the protein structure (21). Similarly nmr studies of GlcNAc and $(GlcNAc)_3$ binding found restricted conformational mobility in the active site region as compared with the free enzyme (22).

The results of the present study of binding $(GlcNAc)_3$ to lysozyme are consistent with a tightening of the structure in the hydrophobic box region of the enzyme (smaller value of θ_0 upon binding), and an increase in the constraining energy (V_0). The increase in the constraining energy from 2.8 to 3.6 kcal/mol upon $(GlcNAc)_3$ binding gives a quantitative feel for the magnitude of the structural changes in the enzyme that are induced.

The lack of detailed information about the structure of the lysozyme-eosin complex makes it difficult to progress quantitatively beyond this observation. Using a molecular graphics docking program to simulate space-filling models of lysozyme and eosin, we observed a pocket in the hydrophobic box region of a reasonable size for accommodating the eosin, with Tyr20 and Tyr23 in favorable positions for hydrogen bonding with the xanthene oxygens on the dye. It is possible that by using a molecular mechanics force-field with the initial configuration determined by graphic docking, one could find a unique minimum energy structure for the binary complex. Then, to estimate the change in the potential of mean force for hindered motion of the eosin upon binding of inhibitor, i.e., to estimate theoretically the potential we have measured in these experiments, one could calculate the free energy for angular excursions of the eosin using molecular dynamics or Monte Carlo techniques. While such theoretical techniques are now just beginning to be applied to large protein systems (36), improvements in computer technology should soon make them routine. It is hoped that from the

interplay between experiments such as the one described and theoretical calculations that a more complete picture of protein dynamics will emerge.

We thank Professor David Oxtoby for a very helpful discussion and Professor James Longworth for a useful suggestion.

This work was supported by grants from SOHIO and the National Science Foundation.

Received for publication 7 January 1986 and in final form 14 March 1986.

REFERENCES

1. Pain, R. H. 1983. Dynamic proteins. *Nature (Lond.).* 305:581–582.
2. Karplus, M., and A. J. McCammon. 1981. The internal dynamics of globular proteins. *CRC Crit. Rev. Biochem.* 9:293–349.
3. Williams, R. J. P. 1978. Energy states of proteins, enzymes and membranes. *Proc. R. Soc. Lond. B. Biol. Sci.* 200:353–380.
4. Gurd, F. R. N., and T. M. Rothgeb. 1979. Motions in proteins. *Adv. Proc. Chem.* 33:73–165.
5. Debrunner, P. G., and H. Frauenfelder. 1982. Dynamics of proteins. *Annu. Rev. Phys. Chem.* 33:283–299.
6. Careri, G., P. Fasella, and E. Gratton. 1979. Statistical time events in enzymes: a physical assessment. *Annu. Rev. Biophys. Bioeng.* 8:69–164.
7. Artymiuk, P. J., C. C. F. Blake, D. E. P. Grace, S. J. Oatley, D. C. Phillips, and M. E. Sternberg. 1979. Crystallographic studies of the dynamic properties of lysozyme. *Nature (Lond.).* 280:563–568.
8. Warshel, A. 1984. Dynamics of enzymatic reacitons. *Proc. Natl. Acad. Sci. USA.* 81:444–448.
9. Frauenfelder, H., G. A. Petsko, and D. Tsernoglou. 1979. Temperature dependent x-ray diffraction as a probe of protein structural dynamics. *Nature (Lond.).* 280:558–563.
10. Munro, I., I. Pecht, and L. Stryer. 1979. Subnanosecond motions of tryptophan residues in proteins. *Proc. Natl. Acad. Sci. USA.* 76:56–60.
11. Tran, C. D., and G. S. Beddard, and A. D. Osborne. 1982. Secondary structure and dynamics of glucagon in solution. *Biochim. Biophys. Acta.* 709:256–264.
12. Delepierre, M., C. M. Dobson, J. C. Hoch, E. T. Olejniczak, F. M. Poulsen, R. G. Ratcliffe, and C. Redfield. 1981. Structures and dynamics of proteins by proton NMR: applications of nuclear Overhauser effects ot lysozyme. *In* Biomolecular Stereodynamics. R. H. Sarma, editor. Adenine Press Inc., Guilderland, New York. 237–253.
13. Olejniczak, E. T., F. M. Poulsen, and C. M. Dobson. 1981. Proton nuclear Overhauser effects and protein dynamics. *J. Am. Chem. Soc.* 103:6574–6580.
14. Chang, M. C., A. J. Cross, and G. R. Fleming. 1983. Internal dynamics and overall motion of lysozyme studied by fluorescence depolarization of the eosin lysozyme complex. *J. Biomol. Struct. & Dyn.* 1:299–318.
15. Kepka, A. G., and L. I. Grossweiner. 1973. Photodynamic inactivation of lysozyme by eosine. *Photochem. Photobiol.* 18:49–61.
16. Baugher, J. F., L. I. Grossweiner, and C. Lewis. 1974. Intermolecular energy transfer in the lysozyme-eosin complex. *J. Chem. Soc. Faraday. II.* 70:1389–1398.
17. Rupley, J. A., L. Butler, M. Gerring, F. J. Hartgenen, and R. Pecoram. 1967. Studies on the enzymatic activity of lysozyme III. The binding of saccharides. *Proc. Natl. Acad. Sci. USA.* 57:1088–1095.
18. Lipari, G., and A. Szabo. 1982. Model-free approach to the interpretation of nuclear magnetic resonance relaxation in molecules. 2. Analysis of experimental results. *J. Am. Chem. Soc.* 104:4559–4570.
19. Kinoshita, K. Jr., S. Kawato, and A. Ikegami. 1977. A theory of fluorescence polarization decay in membranes. *Biophys. J.* 20:289–305.
20. Kinoshita, K. Jr., R. Kataoka, Y. Kimura, O. Gotoh, and A. Ikegami. 1981. Dynamic structure of biological membranes as probed by 1,6-Dipheny-1,3,5-hexatriene: A nanosecond fluorescence depolarization study. *Biochemistry.* 20:4270–4277.
21. Wickett, R. R., G. J. Ide, and A. Rosenberg. 1974. A hydrogen-exchange study of lysozyme conformation changes induced by inhibitor binding. *Biochemistry.* 13:3273–3277.
22. Campbell, I. D., C. M. Dobson, and R. J. P. Williams. 1975. Proton magnetic resonance studies of the tyrosine residues of hen lysozyme-assignment and detection of conformational mobility. *Proc. R. Soc. Lond. B. Biol. Sci.* 189:503–509.
23. Robbins, R. J., G. R. Fleming, G. S. Beddard, G. W. Robinson, P. J. Thistlewait, and G. J. Woolfe. 1980. Photophysics of aqueous tryptophan pH and temperature effects. *J. Am. Chem. Soc.* 102:6271–6279.
24. Chang, M. C., S. H. Courtney, A. J. Cross, R. J. Gulotty, J. W. Petrich, and G. R. Fleming. 1985. Time-correlated single photon counting with microchannel plate detectors. *Anal. Instrum.* 14:433–464.
25. Cross, A. J. and G. R. Fleming. 1984. Analysis of time-resolved fluorescence anisotropy decays. *Biophys. J.* 46:45–56.
26. Tao, T. 1969. Time-dependent fluorescence depolarization and Brownian rotational diffusion coefficients of macromolecules. *Biopolymers.* 8:609–632.
27. Ehrenberg, M., and R. Rigler. 1972. Polarized fluorescence and rotational Brownian motion. *Chem. Phys. Lett.* 14:593–544.
28. Chuang, T. J., and K. B. Eisenthal. 1972. Theory of fluorescence depolarization by anisotropic rotational diffusion. *J. Chem. Phys.* 57:5094–5094.
29. Belford, G. G., R. L. Belford, and G. Weber. 1972. Dynamics of fluorescence polarization in macromolecules. *Proc. Natl. Acad. Sci. USA.* 69:1392–1393.
30. Gavish, B. 1981. Modelling the unusual temperature dependence of atomic displacements in proteins by local nonharmonic potentials. *Proc. Natl. Acad. Sci. USA.* 78:6868–6872.
31. Abramowitz, M., and I. A. Stegun. 1972. Handbook of Mathematical Functions. U.S. Government Printing Office, Washington.
32. Imoto, T., L. N. Johnson, A. C. T. North, D. C. Phillips, and J. A. Rupley. 1972. Vertebrate lysozymes. *In* The Enzymes. Volume 8. P. D. Boyer, editor. Academic Press Inc., New York. 666–868.
33. Schramm, S., and E. Oldfield. 1983. Nuclear magnetic resonance studies of amino acids and proteins. Rotational correlation times of proteins by deuterium nuclear magnetic resonance spectroscopy. *Biochemistry.* 22:2908–2913.
34. Wilbur, D. J., R. S. Norton, A. O. Clouse, R. Addleman, and A. Allerhand. 1976. Determination of rotational correlation times of proteins in solution from carbon-13 spin-lattice relaxation measurements. Effect of magnetic field strength and anisotropic rotation. *J. Am. Chem. Soc.* 98:8250–8254.
35. Dill, K., and A. J. Allerhand. 1979. Small errors in C-H bond lengths may cause large error in rotational correlation times determined from Carbon-13 spin-lattice relaxation measurements. *J. Am. Chem. Soc.* 101:4376–4378.
36. Wooten, J. B., and J. S. Cohen. 1979. Protein mobility and self-association by deuterium nuclear magnetic resonance. *Biochemistry.* 18:4188–4191.
37. Levy, R. M., D. Perahia, and M. Karplus. 1982. Molecular dynamics of an α-helical polypeptide: temperature dependence and deviation from harmonic behavior. *Proc. Natl. Acad. Sci. USA.* 79:1346–1350.
38. Hermans, J., editor. 1985. Molecular Dynamics and Protein Structure: Proceedings of a Workshop held 13–18 May 1984 at the University of North Carolina. Polycrystal Book Service, Western Springs, Illinois.